Ion Channel Stabilization of Synthetic Alamethicin Analogs by Rings of Inter-Helix H-Bonds

Gérard Molle, Jean-Yves Dugast, Gérard Spach, and Hervé Duclohier
Institut Fédératif de Recherches Multidisciplinaires sur les Peptides, URA 500 CNRS-Université de Rouen, 76821 Mont-Saint-Aignan, France

ABSTRACT Rings of inter-helix H-bonds due to Gln at position 7, a highly conserved residue in all pore-forming peptaibols, have been suggested to play an important role in the stabilization of alamethicin channels. In an attempt to test this hypothesis, experimental studies have been undertaken on four synthetic alamethicin non-Aib analogs (Alm-dUL) in which the Gln at position 7 (Q7) is substituted by Ala, Asn, or Ser (Q7A, Q7N, or Q7S). Voltage-dependent pore formation by these analogs in planar lipid bilayers is compared at the macroscopic and single-channel conductance levels. As anticipated, the Q7A substitution abolished all channel-forming activity. The voltage dependence of macroscopic current-voltage curves was conserved with the Q7N substitution but reduced in the Q7S analog. Normalized single-channel conductance ratios between substates follow the same pattern, with the Q7S analog yielding the highest unit conductances. Channel lifetimes were the most significantly modulated parameter with markedly faster kinetics when Gln or Asn was replaced by Ser. The effect of the Q7S substitution on channel lifetimes may be explained through a reduced stabilization of bundles by inter-helix H-bonds.

INTRODUCTION

Ever since the demonstration of excitability phenomena induced by alamethicin in planar lipid bilayers by Mueller and Rudin in 1968 (recently reevaluated by Duclohier and Spach, 1992, and by Rink et al., 1994), this antimicrobial peptaibol has been the object of intensive experimental and theoretical investigations. The pioneering demonstration of single-channel substates by Gordon and Haydon (1972) and the statistical analysis of Boheim (1974) resulted in the proposal by Baumannn and Mueller (1974) that membrane conduction arose from aggregates of amphipathic alamethicin helices (for reviews see, e.g., Latorre and Alvarez, 1981; Spach et al., 1989; Wolley and Wallace, 1992; Sansom, 1993; Cafiso, 1994). The value of alamethicin as a model for voltage-gated ion channels was also advocated by Hall et al. (1984) in light of the crystallographic structure determination of alamethicin monomers by Fox and Richards (1982).

Alamethicin is largely monomeric in lipid bilayers in the absence of an applied membrane potential (Barranger-Mathys and Cafiso, 1994). The "barrel-stave" model now appears as the simplest explanation for alamethicin conduction properties in planar lipid bilayers and, by extension, for similar pore-forming activity induced by other amphipathic natural or synthetic peptides or toxins (Sansom, 1991). Two aspects of the alamethicin structure have been suggested to be of particular functional significance: a) the helix kink induced by Pro14 and b) the Gln7 side chains. Interestingly, both residues are highly conserved in all pore-forming peptaibols (see Katz et al., 1985; Brückner et al., 1985; Rebuffat et al., 1989, 1991, 1992, and Iida et al., 1990). The functional importance of the proline-induced kink has been explored by Duclohier et al. (1992), and the structural consequences of its abolition have been investigated in the nuclear magnetic resonance (NMR) studies of Brachais et al. (1995b). Concerning Gln7, it was suggested by Fox and Richards (1982) that its side chain could stabilize channel formation by enabling inter-helix H-bonding. Indeed, Gln7 lies halfway down the N-terminal (1–14) helical segment and is presumed to be oriented toward the channel lumen. It was suggested to form a "hydrated annulus" that would stabilize the helix bundle and form a constriction of the transbilayer pore. The aim of the current studies is an attempt to verify this proposed role.

Highly voltage-dependent channels similar to alamethicin (albeit with faster kinetics) are preserved in a synthetic peptide (Alm-dUL, for des-Aib-Leu-alamethicin) in which all the Aibs (U, α-amino-isobutyric acid) of alamethicin are replaced by leucines (Molle et al., 1988). To test the influence of Gln7 on the formation and the stabilization of ion channel aggregates, new Alm-dUL peptides in which Gln7 is replaced by alanine (Q7A), serine (Q7S), or asparagine (Q7N) have been synthesized (see the amino acid sequences below) and tested for their conduction properties in planar lipid bilayers, at both the macroscopic and single-channel levels.

Received for publication 12 April 1995 and in final form 15 December 1995.

Address reprint requests to Dr. Gérard Molle, Institut Fédératif de Recherches Multidisciplinaires sur les Peptides, URA 500 CNRS-Université de Rouen, Boulevard M. de Broglie, 76821 Mont-Saint-Aignan, France. Tel.: 33-35-14-67-05; Fax: 33-35-14-67-04; E-mail: gerard.molle@univ-rouen.fr.

0006-3495/96/04/1669/07 $2.00

MATERIALS AND METHODS

Peptide synthesis

Peptides were prepared by the solid-phase technique (Merrifield, 1963) on an Applied Biosystems model 433 A automatic synthesizer. The *tert*-butoxycarbonyl (Boc) was used for temporary Nα protection of amino acids and the OBzl group for the side-chain of Glu.

```
                1                   7                  14                  20
Alm-dUL:  Ac-Leu-Pro-Leu-Ala-Leu-Ala-Gln-Leu-Val-Leu-Gly-Leu-Leu-Pro-Val-Leu-Leu-Glu-Gln-Pheol
"  Q7A:   Ac-Leu-Pro-Leu-Ala-Leu-Ala-Ala-Leu-Val-Leu-Gly-Leu-Leu-Pro-Val-Leu-Leu-Glu-Gln-Pheol
"  Q7N:   Ac-Leu-Pro-Leu-Ala-Leu-Ala-Asn-Leu-Val-Leu-Gly-Leu-Leu-Pro-Val-Leu-Leu-Glu-Gln-Pheol
"  Q7S:   Ac-Leu-Pro-Leu-Ala-Leu-Ala-Ser-Leu-Val-Leu-Gly-Leu-Leu-Pro-Val-Leu-Leu-Glu-Gln-Pheol
```

Briefly, in the protocol described elsewhere (Molle et al., 1989) and modified to yield the amino-alcohol at the C-terminus (Molle and Dugast, 1990), *t*-Boc-Pheol was first esterified with succinic anhydride and then coupled to the benzhydrylamino resin reticulated by 1% divinylbenzene. The synthesis proceeded stepwise toward the N-terminus using 1-hydroxybenzotriazole and *N,N'*-dicyclohexylcarbodiimide as coupling co-reagents. The Nα-Boc was removed at each cycle with trifluoroacetic acid (30% in CH_2Cl_2), and the peptide resin was neutralized by diisopropylethylamine (10% in CH_2Cl_2) before coupling the subsequent aminoacid. After completion of the synthesis and acetylation of the N-terminus, the peptides were released from the resin by alkaline hydrolysis, and for the Q7S analog, the side-chain protecting group (OBzl) was eliminated by the standard HF treatment.

HPLC purification, FAB mass characterization, and circular dichroism

Lyophilized raw products were purified by high-performance liquid chromatography (LKB System, series 2100; Pharmacia LKB Biotechnology, Bromma, Sweden) through repeated steps on a reverse-phase semipreparative column (C_{18}, 10 μm, 8 × 300 mm), from Société Française Chromato Colonne/Shandon Scientific (Eragny, France) under acetonitrile/H_2O gradients.

Electrospray and fast atomic bombardment (FAB) positive ion mass spectrometries allowing an unambiguous characterization of the purified peptides were carried out, respectively, at the laboratory of mass spectrometry of Strasbourg (Centre de Neurochimie, Université Louis Pasteur) and at the Service Central d'Analyses du CNRS (Solaize, France).

Circular dichroism spectra of the peptides in methanol (Sigma, spectroscopic grade) solution were recorded on a spectropolarimeter (Dichrograph Mark V; Jobin-Yvon, Longjumeau, France) using a 0.1-mm quartz cell. Multiple scans between 190 and 300 nm were averaged, and conformational contents were estimated from peak intensities at six selected wavelengths using ellipticity standards based on 15 proteins (Chang et al., 1978).

Peptide reconstitution into planar lipid bilayers

In macroscopic conductance experiments, virtually solvent-free lipid bilayers were formed over a 125-μm hole in a 25-μm-thick PTFE (Goodfellow, Cambridge, England) septum sandwiched between two half-glass cells. Lipid films were spread on top of electrolyte solutions (1 M KCl, 10 mM HEPES, pH 7.4) in both compartments. Bilayer formation was achieved by lowering and then raising the level in one or both sides (Montal and Mueller, 1972) and was monitored by changes in capacitance. The lipid solution at 5–10 mg/ml in hexane (Fluka, spectroscopic grade) was a neutral mixture: 1-palmitoyl, 2-oleoyl phosphatidylcholine (POPC)/1,2-dioleoylphosphatidylethanolamine (DOPE), 7/3 (w/w). Lipids were purchased from Avanti Polar Lipids (Alabaster, AL) and stored at −74°C. Peptides (from a 10^{-5} M stock solution in methanol) were added with stirring to the *cis* or positive side, according to the usual conventions. Transmembrane currents were fed to a Keithley amplifier (model 427; Cleveland, OH) virtually grounded to the *trans* Ag/AgCl electrode. Current-voltage curves were recorded from an *X-Y* plotter.

In single-channel experiments, lipid bilayers were formed at the tip of fire-polished patch-clamp pipettes (Hanke et al., 1984) pulled in two steps (model PP-83; Narishige, Tokyo, Japan) from Vitrex borosilicate tubes (Modulohm, Herlev, DK). The outer tip diameter was about 1 μm, and its resistance in the standard solution used for conductance measurements described above was on the order of 5 MΩ. The same neutral lipids as in macroscopic conductance experiments, but at 0.5-2 mg/ml in hexane, were allowed to evaporate on top of 2 ml of the electrolyte solution in a glass beaker (spreading area: 3 cm^2). To form bilayers, either the pipette was withdrawn and then slowly dipped again or a lipid droplet was applied to the pipette shank. All planar bilayer experiments were performed at 10°C. A programmable waveform generator (SMP 310 model) and a patch-clamp amplifier (RK-300), both from Bio-Logic (Claix, France) were used to record single-channel currents. The latter were fed to an 8-pole low-pass filter and stored on a digital tape recorder (respectively, AF 180 and DTR 1200 models from Bio-Logic). Digitized signals were subsequently analyzed using the Satori v. 3.01 software from Intracel (Royston, England).

RESULTS

Synthesis, purification, and characterization of non-Aib analogs of alamethicin

After solid-phase synthesis and release from the resin, the crude peptides were purified by reverse-phase HPLC. Their purity was checked (98%) by analytical HPLC, and correct primary structures were ascertained by mass spectrometry. As seen in Table 1, there is a good agreement between the theoretical molecular (M), (M + Na) and FAB-derived masses $(M + H)^+$, $(M + Na)^+$. Furthermore, examination of fragmentation patterns confirms the expected sequences (see, e.g., for Alm-dUL, Brachais et al., 1995a).

The secondary structure of Alm-dUL has already been determined and compared with that of alamethicin, and of a derivative in which Pro14 is replaced by Ala, using circular dichroism, Fourier transform infrared spectroscopy, and H-NMR (Brachais et al., 1995b). The helical content of Alm-dUL in methanol is similar to that of alamethicin, albeit a bit higher (55% versus 49%). Molecular modeling based on NMR data would point to a distribution of the kink angles (between the N-terminal helical and the C-terminal segments) up to 30°. Furthermore, the NOE pattern showed almost exclusively an α-helical conformation in the case of Alm-dUL and no evidence for the short 3_{10} (4→1 hydrogen bonds) helical regions, which can make up to 15% of the alamethicin molecule (Fox and Richards, 1982).

TABLE 1 Expected and experimental masses of the analogs

	Experimental		Expected	
Peptide	$(M + H)^+$	$(M + Na)^+$	M	M + Na
Alm-dUL	2188.3	2210.3	2187.4	2210.4
Alm-dUL Q7A		2154.4	2131.7	2154.7
Alm-dUL Q7S	2148.3	2170.2	2147.7	2170.7
Alm-dUL Q7N		2197.2	2174.7	2197.7

Functional assays in planar lipid bilayers

Macroscopic conductances

Peptides were incorporated (via partitioning from a stock solution added to the *cis* side) into POPC/DOPE (7:3) planar lipid bilayers formed according to the Montal and Mueller technique. After allowing typically 15–20 min, during which its capacitance was checked, the bilayer was submitted to a repetitive triangular voltage ramp (typically ± 100 mV·min^{-1}, slow enough for steady-state). Highly asymmetric (positive and negative voltages for a given reference conductance were, e.g., +80 versus −160 mV and +45 vs −140 mV) current-voltage (*I-V*) curves were recorded and superimposed to ensure equilibrium was reached. Fig. 1 compares the macroscopic (hundreds of channels) *I-V* curves for the analogs at two aqueous peptide concentrations (only the positive quadrants are shown). Except for the Q7A analog, which did not yield any significant conductance, Alm-dUL-Q7X analogs induced typical "alamethicin-like" voltage-dependent macroscopic conductance. The development of exponential branches occurred above a threshold that was dependent upon the peptide concentration in the bath.

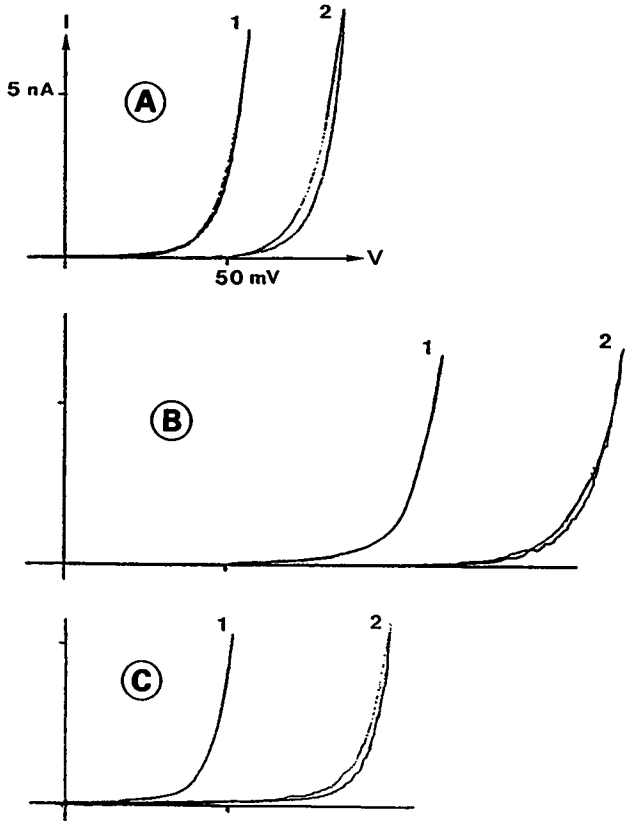

FIGURE 1 Macroscopic current-voltage curves for Alm-dUL (*A*) compared to Q7S (*B*) and Q7N (*C*) analogs at two aqueous peptide concentrations (*cis*-side): 5 10^{-8} M (*curves 2*) and 10^{-7} M (*curves 1*). For each curve, 3 to 5 sweeps (at about 5 mV/s) were superimposed. Electrolyte solution: both sides of a POPC:DOPE (7/3) bilayer: 1 M KCl, 5 mM HEPES (pH: 7.4). T = room temperature.

TABLE 2 Macroscopic conductance parameters yielding the concentration-dependence (V_a), the voltage dependence (V_e), and the apparent mean number (N_{App}) of peptide molecules involved in the channels

Peptide	V_a (mV)	V_e (mV)	N_{App}	$N_{Rounded}$
Alm-dUL	48 ± 4	8.0 ± 0.3	6.0 ± 0.2	6
Q7S	74.5 ± 5	11.1 ± 0.2	6.8 ± 0.2	7
Q7N	63.5 ± 5	6.9 ± 0.2	9.1 ± 0.6	9

This direct screening already highlights the significantly different responses induced by the Q7S derivative: at concentrations similar to those for the other two analogs, activation thresholds are higher and the steepness of the current is reduced. As anticipated from its side chain (amide group), the behavior of Alm-dUL-Q7N is much closer to that of the parent molecule.

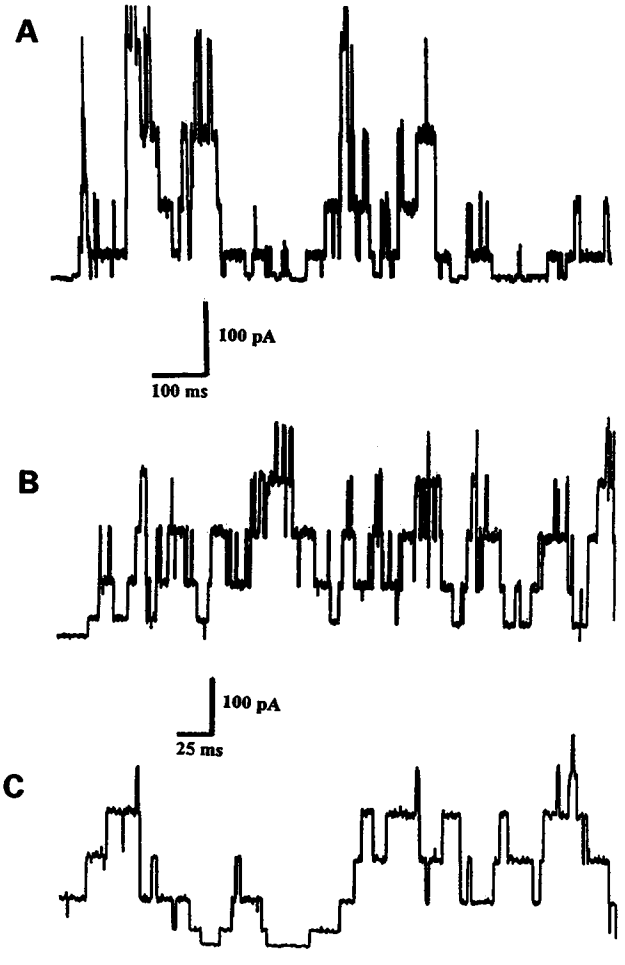

FIGURE 2 Representative single-channel current traces induced by Alm-dUL (*A*) and Q7N analog (*B*), (*C*) being an enlarged section of the latter. Identical scale bars (time base 100 ms) apply for *A* and *B*. Openings are upward transitions. Applied voltage was 140 mV throughout. Bessel filter during acquisition: 10 kHz, digitally refiltered at 1–3 kHz for plotting and data treatment. Symmetrical electrolyte solutions and lipid composition of tip-dip bilayers were the same as described for Fig. 1, except that 1 mM $CaCl_2$ was added to improve the patch seal. T = 10°C.

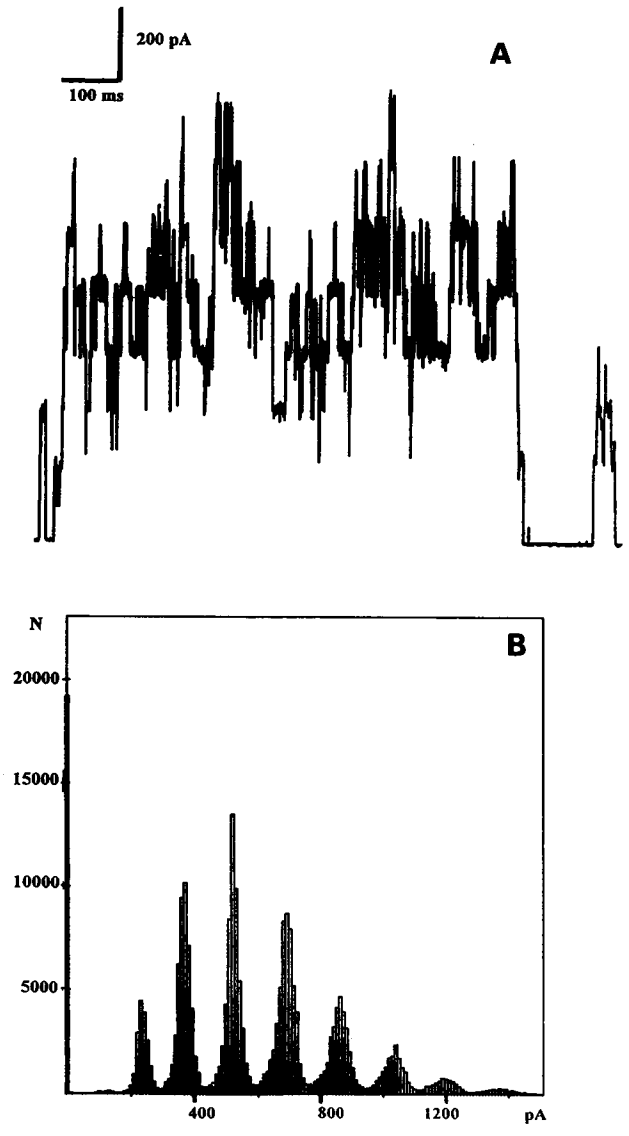

FIGURE 3 (*A*) Example of high conductance levels displayed by Alm-dUL-Q7S (140 mV). (*B*) Single-channel amplitude histogram derived from a 1-s section of the above.

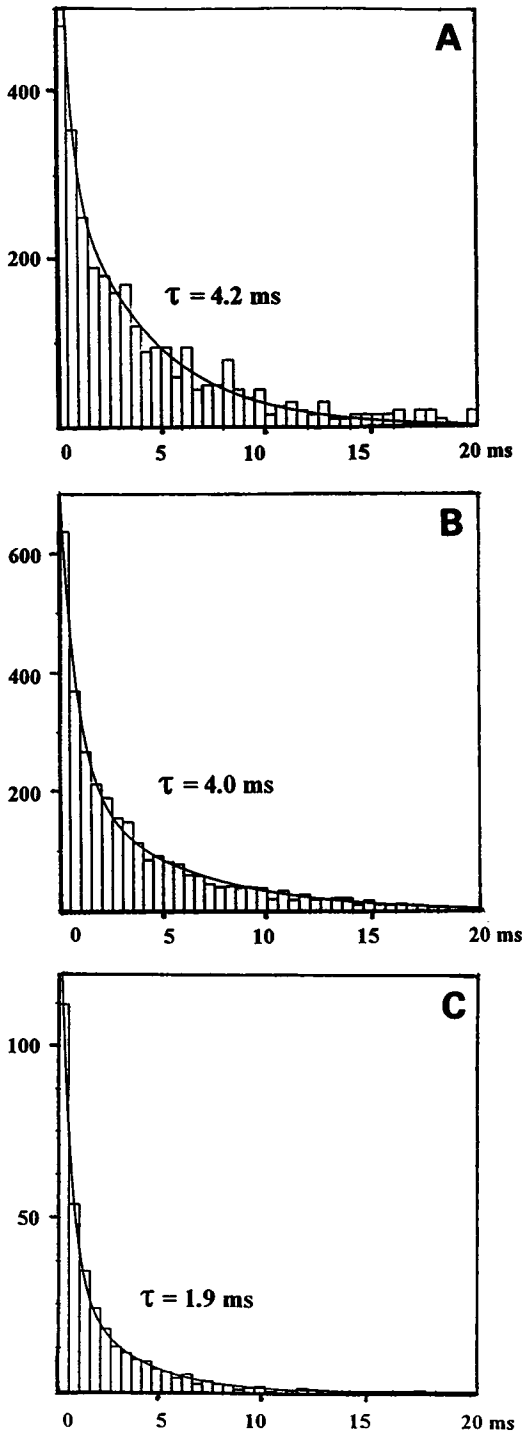

FIGURE 4 Open dwell time histograms (examples for the most probable substate) compared between Alm-dUL (*A*) and the Q7N (*B*) and Q7S (*C*) analogs. The mean "open lifetime" (best fit to a single exponential) is indicated for each analog and this particular substate. Applied voltage, 140 mV.

As demonstrated for alamethicin and based on the fact that the peptide-induced conductance in steady-state is both a power function of concentration and an exponential function of voltage (Hall et al., 1984), N_{App}, the apparent mean number of monomers involved in the conducting aggregates, can be derived as the ratio $N_{App} = V_a/V_e$. V_a is the voltage shift of thresholds produced by an e-fold change in peptide aqueous concentration and V_e is the voltage increment resulting in an e-fold change in conductance. Table 2 shows that a high voltage dependence (V_e) is preserved with the Q7N substitution but reduced for Q7S, whereas the apparent number of monomers is significantly higher with the Q7N substitution, which means that, on the average, states with more monomers are favored when compared with Alm-dUL.

Single-channel conductances

The trends disclosed in the macroscopic analysis are confirmed by the analysis of single-channel experiments. Alm-dUL, Q7S, and Q7N analogs all induce a multistate behav-

TABLE 3 Sublevel conductance values in pS of alamethicin analogs in POPC/DOPE membranes at 130 mV in 1 M KCl

Peptide	1	2	3	4	5	6
Alm-dUL	50	220	700	1350	2230	3260
Q7S	60	240	740	1530	2470	3500
Q7N	40	180	550	1050	1630	2210

Temperature 10°C and peptide concentration in the 10^{-9} M range.

ior like alamethicin, whereas Q7A does not show any channel-forming activity. Fig. 2 compares typical single-channel current traces (at $V = +140$ mV) induced by Alm-dUL and the Q7N analog. Surprisingly, the latter analog yields more sustained activity evenly distributed between substates, whereas higher substates are only reached in bursts in the case of the parent molecule (Alm-dUL). Note that this is in agreement with the increased N_{App} deduced for the Q7N analog from macroscopic conductance data. Furthermore, the replacement of Gln7 by Asn7 gives lower conductance values, and the increments between each level are also lower (see Table 3).

The behavior displayed by Alm-dUL-Q7S was found to be much more erratic. Even after twice as many experiments (i.e., 10) as for the other two analogs, a clear-cut or averaged pattern of single-channel activity did not emerge. Events most often occur in bursts of rapidly fluctuating high levels interspersed with silent periods and low-level activity (see Fig. 3 *A*). Nevertheless, the conductance histogram shown in Fig. 3 *B*, typical for half the experiments, still points out an "alamethicin-like" pattern, i.e., with conductance increments between substates that are increasing. The data presented in Table 3 for this are in line with the other two analogs. Indeed, the normalized ratios of single-channel sublevels are quite comparable for the three analogs: 1:4.4:14:27:45:65 (Alm-dUL); 1:4:12:26:41:58 (Alm-dUL-Q7S); and 1:4.5:14:26:41:55 (Alm-dUL-Q7N). It should be stressed that equal increments between substates, as initially reported for alamethicin by Gordon and Haydon (1975) and more recently by Taylor and de Levie (1991) but with cholesterol-containing bilayers, are not encountered in our experiments before the sixth subconductance level is reached. However, some experiments with the Q7S analog (especially when the voltage is increased) point to equal conductance increments. Thus, the barrel-stave mechanism most likely applies for all three analogs and, at least for the first three or four sublevels (i.e., for bundles of about four to seven helices, see Hanke and Boheim, 1980), Alm-dUL and Q7N appear to be more closely related to each other than to the Q7S analog. Note that from geometrical considerations of the bundle lumen defined as the juxtaposition of the hydrophilic sectors of a variable number of monomers, the area increments and thus the conductance increments are actually increasing with the sequential uptake of monomers (see also Spach et al., 1983).

Channel kinetics are the most significantly modulated parameter when substituting glutamine at position 7 by serine or asparagine. This was already apparent from the hystereses of macroscopic *I-V* curves (Fig. 1) (the narrower the hysteresis, the faster the kinetics) and inspection of single-channel current traces (Figs. 2 and 3 *A*). This is quantified in Fig. 4, which compares examples of open lifetime histograms for the most probable substates at the same voltage for Alm-dUL and the Q7N and Q7S analogs. τ, the mean open lifetime for the most probable substate, is comparable between Alm-dUL and Q7N (4.2 and 4.0 ms, respectively) but significantly reduced (to 1.9 ms) in the Q7S analog. The same applies for the neighboring substates.

DISCUSSION

Glutamine 7 was postulated by Fox and Richards (1982) to be a key residue in the voltage-gated alamethicin channel. In their view, each Q7 side chain may form a H-bond with the same residue on the neighboring helix in the bundle. The second free hydrogen of the amide group could then H-bond with water molecules both below and above the Q7 annulus thus formed. Although the present work (functional data) does not bring direct experimental support to this structural hypothesis, we will examine hereafter arguments that might favor the implication of inter-helix H-bonds in the stabilization of the conducting aggregates formed by amphipathic peptides. The most clear-cut effect is obviously the complete loss of channel activity when glutamine 7 is replaced by alanine, an apolar residue unable to form side-chain H-bonds. Nearly initial functional properties are restored with asparagine 7, despite its side chain being shorter than that of glutamine.

The significantly higher N_{APP} (mean and apparent number of monomers per conducting aggregate) derived for the Q7N analog from macroscopic conductance experiments (Table 2) is in agreement with the higher subconductance levels being more populated for this analog than with the parent molecule Alm-dUL (Fig. 2*B*). In addition the smaller side chain of Asn with still strong H-bonding ability seem associated with smaller single-channel conductance increments (Table 3). It is possible that asparagine-induced interhelical H-bonds might favor tighter bundles which, due to steric hindrance for example, would be destabilized (see the associated kinetics) especially for the lower aggregates. As for Q7S, the substitution of amide bonds (of Gln or Asn) by an hydroxyl group (-CH_2OH of Ser) results in much weaker H-bonds. The less stable Q7S aggregates are correlated with a significantly reduced voltage dependence (Table 2) and shorter lifetimes (Figs. 3*A* and 4*C*): a higher transmembrane voltage is presumably required to favor the conducting parallel helix bundle.

The fact that nonintegral conductance sublevels are still observed for the Q7S analog argues against the proposal by Fox and Richards (1982) that such sublevels result from the sequential breaking of Q7 H-bonds and of the hydrated annulus. Rather, uptake and release of helical monomers continue to provide the better explanation of the data. Of course, such changes in the number of helices per bundle

will require transient perturbation of the H-bonding pattern, if any. If one assumes that the lowest conductance level (~50 pS) corresponds to a $N = 4$ bundle, then the observed conductances of 550 to 750 pS for $N = 6$ and 2200 to 3500 pS for $N = 9$ are in rough quantitative agreement with a geometric model where the lumen is bounded by a variable number of helical rods (Hanke and Boheim, 1980). However, the analysis of channel conductance in terms of pore radius can only be useful for large pores. It provides the correct trend for the bundles with different sizes but cannot account for the variations in the conductance for the different analogs.

The single-channel kinetics compared for Alm-dUL, Q7N, and Q7S channels could also argue for the stabilization of helix bundles by residue 7 possibly mediating inter-helix H-bonds. For all conductance levels, the single-channel lifetime τ is smaller for Alm-dUL-Q7S than for Alm-dUL and Alm-dUL-Q7N. Note that the lifetime differences seem to simply reflect the relative hydrophibicities of the side chains: $\langle H \rangle = -0.85, -0.78, -0.18, 0.62$ (normalized consensus scale of Eisenberg, 1984) for Gln, Asn, Ser, and Ala, respectively. Shorter channel lifetimes may be the result of a lower stability for a given conductance level and/or a lower activation energy barrier for switching between adjacent levels. One may expect that the strength of H-bonding interactions between adjacent helices is considerably reduced for Alm-dUL-Q7S relative to the other two peptides. This is entirely consistent with the interpretation of smaller τ values for Alm-dUL-Q7S if switching between adjacent conductance levels requires insertion/loss of a peptide monomer from the helix bundle. The increased noise level of the open substates of the Q7S analog also argues for a greater destabilization of the bundle geometry on a rapid time scale. The role of the residual inter-helix H-bonding in Alm-dUL-Q7S is emphasized by the loss of channel activity when the Ser is replaced by Ala. Of course, the Q7A substitution may have other channel-inhibiting effects, for example, loss of the central ring of polar side chains necessary for ion permeation, i.e., a significantly reduced amphipathic nature of the peptide and/or stability of parallel helix organization. However, because the Q7A substitution does enhance the average hydrophobicity of the peptide, the latter certainly interacts with the bilayer with some probability to form aggregates that might not be conducting because of the unfavorable energetic barrier to ion transfer provided by alanines. Indeed, these aggregates are still likely to be stabilized by the Gln 18 "ring" and the associated inter-helix H-bonds and a strong helix-helix hydrophobic interaction, particularly between Ala 3 and Val 15 (Molle et al., 1993).

In summary, the experimental data suggest that a) helix bundles of varying sizes corresponding to the different conductance levels remain the simplest working model, not invalidated by the present study, and b) Gln 7 is indeed a key-residue, possibly forming inter-helix H-bonds that may have a role in the stabilization of channel-forming helix bundles. On this basis, it is worthwhile attempting to undertake Alm-dUL-Q7X channel modeling, via inclusion of intra-pore solvent, lipid bilayer and transbilayer voltage difference, to have a better understanding at the molecular level of the relationship between structure and function in this important group of channel models.

We are indebted to CEB-Rouen (E. Bernardi, A. R. Schoofs) for peptide synthesis facilities and to M. Lucaciu (University of Cluj-Napoca, Rumania) for participating in the macroscopic conductance experiments. We also thank J. Breed, I. D. Kerr, and M. S. P. Sansom (Laboratory of Molecular Biophysics, Oxford University) for interesting discussions.

This work was supported by GdR 1153 CNRS "Peptides et Protéines Amphipatiques."

REFERENCES

Barranger-Mathys, M., and D. S. Cafiso. 1984. Collisions between helical peptides in membranes monitored using electron paramagnetic resonance: evidence that alamethicin is monomeric in the absence of a membrane potential. *Biophys. J.* 67:172–176.

Baumann, G., and P. Mueller. 1974. A molecular model of membrane excitability. *J. Supramol. Struct.* 2:538–557.

Boheim, G. 1974. Statistical analysis of alamethicin channels in black lipid membranes. *J. Membr. Biol.* 19:277–303.

Brachais, L., D. Davoust, and G. Molle. 1995a. Conformational study of a synthetic analogue of alamethicin: influence of the conformation on ion channels lifetimes. *Int. J. Pept. Protein Res.* 45:164–172.

Brachais, L., H. Duclohier, C. Mayer, D. Davoust, and G. Molle. 1995b. Influence of proline-14 substitution on the seconday structure in a synthetic analogue of alamethicin. *Biopolymers.* 36:547–558.

Brückner. H., W. A. König, M. Aydin, and G. Jung. 1985. Trichotoxin A-40. Purification by counter-current distribution and sequencing of isolated fragments. *Biochim. Biophys. Acta.* 827:51–62.

Cafiso, D. S. 1994. Alamethicin: a peptide model for voltage-gating and protein-membrane interactions. *Annu. Rev. Biophys. Biomol. Struct.* 23:141–165.

Chang, C. T., C.-S. C. Wu, and J. T. Yang. 1978. Circular dichroism analysis of protein conformation: inclusion of the β-turns. *Anal. Biochem.* 91:13–31.

Duclohier, H., G. Molle, J.-Y. Dugast, and G. Spach. 1992. Prolines are not essential residues in the "barrel-stave" model for ion channels induced by alamethicin analogues. *Biophys. J.* 63:868–873.

Duclohier, H., and G. Spach. 1992. The negative resistance induced by alamethicin and basic polypeptides: sensitivity to TTX, modulation by divalent cations and correlations with conformational changes. *Biophys. J.* 61:A115.

Eisenberg, D. 1984. Three-dimensional structure of membrane and surface proteins. *Annu. Rev. Biochem.* 53:595–623.

Fox, R. O., and F. M. Richards. 1982. A voltage-gated ion channel model inferred from the crystal structure of alamethicin at 1.5 Å resolution. *Nature.* 300:325–330.

Gordon, L. G. M., and D. A. Haydon. 1972. The unit conductance channel of alamethicin. *Biochim. Biophys. Acta.* 255:1014–1018.

Gordon, L. G. M., and D. A. Haydon. 1975. Potential-dependent conductances in lipid membranes containing alamethicin. *Phil. Trans. R. Soc. Lond. B.* 270:433–447.

Hall, J. E., I. Vodyanoy, T. M. Balasubramanian, and G. R. Marshall. 1984. Alamethicin: a rich model for channel behavior. *Biophys. J.* 45:233–247.

Hanke, W., and G. Boheim. 1980. The lowest conductance state of the alamethicin pore. *Biochim. Biophys. Acta.* 596:456–462.

Hanke, W., C. Methfessel, H. U. Wilmsen, and G. Boheim. 1984. Ion channel reconstitution into planar lipid bilayers on glass pipettes. *Biochem. Bioenerg. J.* 12:329–339.

Iida, A., M. Okuda, S. Uesato, Y. Takaishi, T. Shingu, M. Morita, and T. Fujita. 1990. Fungal metabolites. Part 3. Structural elucidation of antibiotic peptides, Trichosporin-B-IIIb, -IIIc, -IVb, -IVc, IVd, -VIa and -VIb from *Trichoderma polysporum*. Application of fast-atom bombardment mass spectrometry/mass spectrometry to peptides containing a

unique Aib-Pro peptide bond. *J. Chem. Soc. Perkin. Trans.* 1990: 3249–3255

Katz, E., M. Aydin, N. Lucht, W. A. König, T. Ooka, and G. Jung. 1985. Sequence and conformation of Suzukacillin A. *Liebigs Ann. Chem.* 1985:1041–1062.

Latorre, R., and O. Alvarez. 1981. Voltage-dependent channels in planar lipid bilayer membranes. *Physiol. Rev.* 61:77–150.

Merrifield, R. B. 1963. Solid phase peptide synthesis. I. The synthesis of a tetrapeptide. *J. Am. Chem. Soc.* 89:2149–2154.

Molle, G., H. Duclohier, J.-Y. Dugast, and G. Spach. 1989. Design and conformation of non-Aib synthetic peptides enjoying alamethicin-like ionophore activity. *Biopolymers.* 28:273–283.

Molle, G., H. Duclohier, J.-Y. Dugast, and G. Spach. 1993. Influence of helix-helix contacts on the stability of ion channels induced by a synthetic analogue of alamethicin. *In* Peptides 1992. C. H. Schneider and A. N. Eberle, editors. ESCOM Science Publishers, Leiden. 917–918.

Molle, G., and J.-Y. Dugast. 1990. Synthèse sur support solide de peptides comportant un résidu aminoalcool C-terminal. *Tetrahedron Lett.* 31: 6355–6356.

Molle, G., J.-Y. Dugast, H. Duclohier, and G. Spach. 1988. Conductance properties of des-Aib-Leu-des-Pheol-Phe-alamethicin in planar lipid bilayers. *Biochim. Biophys. Acta.* 938:310–314.

Montal, M., and P. Mueller. 1972. Formation of bimolecular membranes from monolayers and study of their properties. *Proc. Natl. Acad. Sci. USA.* 69:3561–3566.

Mueller, P., and D. O. Rudin. 1968. Action potentials induced in bimolecular lipid membranes. *Nature.* 217:713–719.

Rebuffat, S., H. Duclohier, C. Auvin-Guette, G. Molle, G. Spach, and B. Bodo. 1992. Membrane-modifying properties of the pore-forming peptaibols saturisporin SA IV and harzianin HA V. *FEMS Microbiol. Immunol.* 105:151–160.

Rebuffat, S., M. El Hajji, P. Hennig, D. Davoust, and B. Bodo. 1989. Isolation, sequence, and conformation of seven trichorzianines B from *Trichoderma harzianum. Int J. Peptide Protein Res.* 34:200–210.

Rebuffat, S., Y. Prigent, C. Auvin-Guette, and B. Bodo. 1991. Trichologins BI and BII, 19-residue peptaibols from *Trichoderma longibrachiatum.* Solution structure from two-dimensional NMR spectroscopy. *Eur. J. Biochem.* 201:661–674.

Rink, T., H. Bartel, G. Jung, W. Bannwarth, and G. Boheim. 1994. Effects of polycations on ion channels formed by neutral and negatively charged alamethicins. *Eur. Biophys. J.* 23:155–165.

Sansom, M. S. P. 1991. The biophysics of peptide models of ion channels. *Prog. Biophys. Mol. Biol.* 55:139–235.

Sansom, M. S. P. 1993. Structure and function of channel-forming peptaibols. *Q. Rev. Biophys.* 26:365–421.

Spach, G., H. Duclohier, G. Molle, and J-M. Valleton. 1989. Structure and supramolecular architecture of membrane channel-forming peptides. *Biochimie.* 71:11–21.

Spach, G., F. Heitz, and Y. Trudelle. 1983. Peptides forming ion pores in bilayer lipid membranes. *In* Physical Chemistry of Transmembrane Ion Motions. G. Spach, editor. Elsevier Publishers B. V., Amsterdam. 375–383.

Taylor, R. J., and R. de Levie. 1991. "Reversed" alamethicin conductance in lipid bilayers. *Biophys. J.* 59:873–879.

Wolley, G. A., and B. A. Wallace. 1992. Model ion channels: gramicidin and alamethicin. *J. Membr. Biol.* 129:109–136.